

Bounds on Gauge Bosons Coupled to Non-conserved Currents

Majid Ekhterachian,^{1,*} Anson Hook,^{1,†} Soubhik Kumar,^{2,3,‡} and Yuhsin Tsai^{4,§}

¹*Maryland Center for Fundamental Physics, Department of Physics,
University of Maryland, College Park, MD 20742, USA*

²*Berkeley Center for Theoretical Physics, Department of Physics,
University of California, Berkeley, CA 94720, USA*

³*Theoretical Physics Group, Lawrence Berkeley National Laboratory, Berkeley, CA 94720, USA*

⁴*Department of Physics, University of Notre Dame, IN 46556, USA*

We discuss the unitarity bounds on vectors coupled to currents whose non-conservation is due to mass terms, such as $U(1)_{L_\mu-L_\tau}$. Due to emission of many final state longitudinally polarized gauge bosons, inclusive rates grow exponentially fast in energy, leading to constraints that are only logarithmically dependent on the symmetry breaking mass term. This exponential growth is unique to Stueckelberg theories and reverts back to polynomial growth at energies above the mass of the radial mode. As an example, we demonstrate how the total inelastic cross section of the LHC beats out cosmological bounds to place the strongest limit on Stueckelberg $U(1)_{L_\mu-L_\tau}$ models for most masses below a keV. We also present a stronger, but more uncertain, bound coming from the validity of perturbation theory at the LHC.

INTRODUCTION

Recently, new light weakly coupled particles have increasingly become a focus as either a mediator to a dark sector [1–3], as dark matter itself [4–8], or to explain potential anomalies [9–14]. A particularly well motivated candidate is a vector boson. The currents that these vector bosons couple to can either be conserved, e.g. $U(1)_{B-L}$ with Dirac neutrino masses, or they can be non-conserved, e.g. $U(1)_L$ or $U(1)_{L_\mu-L_\tau}$.

In this letter we will continue a long line of research into the bounds that can be placed on vector bosons coupled to non-conserved currents, see e.g. Refs. [15–22]. As is well known, these models are non-renormalizable field theories and as a result have amplitudes that grow with energy. Eventually these amplitudes grow so large that tree level amplitudes violate unitarity at the energy scale Λ , indicating that perturbation theory has broken down. Requiring that new physics appears below the scale Λ gives the unitarity bound. Unitarity bounds have a long storied history, see e.g. Refs. [23–26], and the famous application to the Higgs boson [27–30].

Typically non-conservation of the currents comes from either mass terms or anomalies and in this letter we will focus on the case of mass terms. Specifying this starting point locks us into considering the Stueckelberg limit of gauge theories¹ as including the radial mode renders mass terms gauge invariant. We will show that a Stueckelberg theory coupled to a non-conserved current has inclusive rates that grow exponentially fast in energy due to multiparticle emission. This exponential growth is unique to the Stueckelberg limit and becomes polynomial at energies above the mass of the radial mode.

We will show that the exponential growth of amplitudes in these models gives extremely strong unitarity bounds that scale as

$$\Lambda \approx \frac{4\pi m_X}{\sqrt{27}g_X} \log^{3/2} \left(\frac{m_X}{g_X m} \right), \quad (1)$$

where g_X and m_X are respectively the coupling and the mass of the gauge boson, and m is the symmetry breaking mass term. To show how strong this unitarity bound is, let us consider the Stueckelberg limit of $U(1)_{L_\mu}$. Typically one assumes that the strongest unitarity bound on this model comes from the fact that this current is anomalous. Redoing the unitarity bound (for details see the Supplementary Material) using our conventions leads to a slightly stronger result than the standard result [15]

$$\Lambda_a = \frac{\sqrt{4\pi}m_X}{g_X} \frac{32\pi^2}{g^2}, \quad (2)$$

where g is the $SU(2)_W$ gauge coupling. Comparing this with Eq. (1) taking $m_X/g_X \simeq 1$ GeV, motivated by our later results, and $m \simeq 0.05$ eV, as the mass of the neutrino, we find that $\Lambda \sim \Lambda_a/10$. This shows that despite the extremely small neutrino mass, its non-zero value still gives a unitarity bound almost an order of magnitude more stringent than the anomaly does! Thus before considering moving to an anomaly free theory such as $U(1)_{L_\mu-L_\tau}$, one should first UV complete the symmetry breaking neutrino mass terms. In contrast, for a Higgsed $U(1)_{L_\mu}$ one can naturally have the exact opposite scenario where $\Lambda_a \ll \Lambda$.

Unitarity in these models is restored by the inclusion of the radial mode. However in these UV completions, the small fermion mass is the result of a higher dimensional operator so that scattering of the radial mode has its own unitarity bound. Constraints on the UV completion are fairly model dependent, however since it is likely that the

¹ The Stueckelberg limit is when the mass of the radial mode is taken to be heavier than the energy scale under consideration.

UV completion only couples to the SM via the neutrino mass term, bounds on it are plausibly fairly weak. On the other hand, for Stueckelberg gauge bosons we obtain robust, model-independent bounds that do not rely on the dynamics of the radial mode. While these bounds can be evaded by going away from the Stueckelberg limit by including the radial mode at sufficiently low energies, the radial mode should then be taken into account whenever processes at energies larger than its mass are studied.

In this letter we will focus on gauge bosons coupled to the lepton number currents, which are only non-conserved because of the extremely small neutrino masses. To find explicit bounds, we consider the total decay width of the W boson and the total inelastic cross section of the Large Hadron Collider (LHC). For more familiar non-renormalizable field theories, such as gauge theories with anomalies or the SM without the Higgs, amplitudes grow as $(\text{energy}/\text{mass})^2$. However in our case, the inclusive cross section grows exponentially in energy/mass, $\sim e^{3(g_X E/4\pi m_X)^{2/3}}$, and thus much more crude constraints, such as the total inelastic cross section of the LHC, are sufficient to place extremely strong bounds.

The bounds we obtain are essentially independent of what the exact model under consideration is, thus in the introduction we will only list our bounds on $U(1)_{L_\mu-L_\tau}$ with Dirac neutrino masses. We find that

$$\frac{m_X}{g_X} > 54 \text{ MeV}; \quad \frac{m_X}{g_X} > 2.3 \text{ GeV} \quad (3)$$

using the total decay width of the W boson and the inelastic cross section of the LHC respectively. In the high mass limit, this is only a factor of ~ 100 weaker than the extremely precise measurements of the $g-2$ of the muon [31, 32]. Meanwhile for $m_X \lesssim 1 \text{ keV}$, this is the strongest constraint on these models beating out even cosmological bounds.²

UNITARITY BOUND

In order to demonstrate the exponential growth of amplitudes, we will consider the toy scenario of a gauge boson coupled to only the left handed piece of a Dirac fermion ν , whose current is not conserved due to explicit breaking by a small Dirac mass term m_ν . Namely we consider a theory with

$$\mathcal{L} = -\frac{1}{4}F_X^2 + i\bar{\nu}(\not{\partial} - ig_X \not{A}_X P_L)\nu - m_\nu \bar{\nu}\nu + \frac{1}{2}m_X^2 A_X^2, \quad (4)$$

where F_X is the field strength of the gauge boson A_X . In the limit of small m_ν , the scale at which perturbation theory breaks down, Λ , is much larger than the mass of the gauge bosons. In this limit, things simplify as the high energy behavior of A_X can be obtained from the Goldstone boson equivalence theorem. Namely, the matrix element obeys $\mathcal{M}(A_X^L + \dots) \approx \mathcal{M}(\phi + \dots)$, where A_X^L is a longitudinally polarized A_X and ϕ is the Goldstone boson.

We obtain the theory with Goldstone bosons by leaving unitarity gauge via a chiral gauge transformation, $\nu_L \rightarrow \exp(ig_X \phi/m_X)\nu_L$. As the mass term is not gauge invariant, it transforms into

$$V = m_\nu \bar{\nu} e^{ig_X P_L \phi/m_X} \nu = \sum_n \bar{\nu} \frac{m_\nu}{n!} \left(\frac{ig_X P_L \phi}{m_X} \right)^n \nu. \quad (5)$$

From this, it is clear that the theory is non-renormalizable and has a UV cutoff. The Goldstone boson equivalence theorem lets us compute the probability of emitting many longitudinal gauge bosons by calculating the much simpler process of emitting many ϕ particles using the above interaction.

As one can see, considering processes involving n ϕ s gives a matrix element $\sim m_\nu (g_X E/m_X)^n$ that becomes more and more insensitive to the small mass parameter m_ν as n becomes larger and larger. This causes the best unitarity bound to come from taking n larger and larger. However, in the large n limit, the $1/n!$ coming from dealing with identical final state particles penalizes taking n too large. Thus the optimal unitarity bound comes from taking an intermediate value of the number of gauge bosons n_{opt} .

A calculation done in the Supplementary Materials shows that the amplitude $\hat{\mathbf{M}}$ of the process $\nu + n\phi \rightarrow \nu + n\phi$ is

$$|\hat{\mathbf{M}}(\nu + n\phi \rightarrow \nu + n\phi)| = \frac{g_X m_\nu}{2m_X(n+1)!n!(n-1)!} \left(\frac{g_X E}{4\pi m_X} \right)^{2n-1} \quad (6)$$

in the limit that $E \gg nm_X$. Unitarity requires that $|\hat{\mathbf{M}}| < 1$. In order to obtain the strongest bounds, we choose the n that maximizes Eq. (6) to obtain in the large n limit

$$|\hat{\mathbf{M}}(\nu + n_{\text{opt}}\phi \rightarrow \nu + n_{\text{opt}}\phi)| \sim \frac{g_X m_\nu}{2m_X} e^{3\left(\frac{g_X E}{4\pi m_X}\right)^{2/3}}. \quad (7)$$

This maximum value of $|\hat{\mathbf{M}}|$ is obtained for $n_{\text{opt}} \approx (g_X E/4\pi m_X)^{2/3}$. Requiring unitarity holds for Eq. (7) gives the leading logarithmic behavior

$$E = \Lambda \approx \frac{4\pi m_X}{\sqrt{27}g_X} \log^{3/2} \left(\frac{m_X}{g_X m_\nu} \right). \quad (8)$$

From this calculation we see the behavior claimed in the introduction. Amplitudes have an exponential

² If the gauge boson instead coupled to L_e , the strongest bounds at low mass are from neutrino oscillations in the earth [33] and it is only for masses $m_X \lesssim 10^{-16} \text{ eV}$ that our bounds win out.

growth in energy and the strongest growth comes from emitting multiple gauge bosons. In this calculation, we made the approximation that the energy carried by each of the A_X gauge bosons is much larger than the mass when we utilized the Goldstone boson equivalence theorem. Combining the expression for n_{opt} with Eq. (8) and the requirement that $E \gg n_{\text{opt}} m_X$, we find that our massless approximation of the unitarity bound is valid when $g_X \lesssim 4\pi\sqrt{\log(m_X/g_X m_\nu)}/3$. In the large log limit, the massless limit is always a valid approximation.

MODELS

We now briefly describe the models under consideration and set up some notation. The results in the next section will be given in the 1-flavor approximation so we will also discuss how to easily take into account the standard 3-flavor set up. For ease of expression, in this section we will use Weyl notation for fermions.

As mentioned before, we will be considering the Stueckelberg limit of different $U(1)$ gauge theories. We first consider $U(1)_{L_\mu-L_\tau}$. We assume Dirac neutrinos and that the right-handed neutrinos are neutral under $L_\mu - L_\tau$. The flavor basis is related to the mass basis by $\nu_F = U\nu_M$, where ν_F (ν_M) are the flavor (mass) basis left handed neutrinos and U is the PMNS matrix. In the flavor basis the neutrino mass term is $\nu^c M_d U^\dagger \nu_F$ where M_d is a diagonal matrix of the neutrino masses $m_{1,2,3}$. To leave unitary gauge, the flavor-basis SM neutrinos are rotated by,

$$\nu_F \rightarrow P\nu_F \quad P = \text{diag}\left(1, e^{+ig_X\phi/m_X}, e^{-ig_X\phi/m_X}\right). \quad (9)$$

Thus the neutrino mass term involving the Goldstone bosons ϕ becomes

$$\begin{aligned} \mathcal{L}_{\nu\text{mass}}^D &= \nu^c M_d U^\dagger P\nu_F + \text{h.c.} \\ &\supset \sum_{n,j} \frac{1}{n!} \left(\frac{ig_X\phi}{m_X}\right)^n \nu_j^c M_{d,j} \left(U_{j\mu}^\dagger \nu_\mu + (-1)^n U_{j\tau}^\dagger \nu_\tau\right). \end{aligned}$$

From this, we see that any 1-flavor process involving n high energy gauge bosons can be converted into the 3-flavor result by replacing

$$m_\nu^2 \rightarrow \sum_{j=1}^3 (|U_{\mu j}|^2 + |U_{\tau j}|^2) m_j^2. \quad (10)$$

The other gauge theory we will consider is $U(1)_L$ with Majorana neutrino masses. In this case, after leaving unitary gauge the mass term is

$$\mathcal{L}_{\nu\text{mass}}^M = e^{2ig_X\phi/m_X} \nu_M^T M_d \nu_M + \text{h.c.} \quad (11)$$

From this, the 1-flavor results can be generalized using the substitution

$$g_X \rightarrow 2g_X, \quad m_\nu^2 \rightarrow \sum_{l=e,\mu,\tau} \sum_{j=1}^3 |U_{lj}|^2 m_j^2. \quad (12)$$

CONSTRAINTS

We now present exclusions coming from the emission of many final state gauge bosons. We will consider two different constraints, the decay of the W boson and the total inelastic cross section of the LHC as well as a more uncertain constraint coming from the validity of perturbation theory at the LHC. Our results will be presented in the simplified 1-flavor model. Eq. (10) and Eq. (12) can be used to convert the results into the two specific models of interest. In particular, in Fig. 1 and Fig. 2 we show the results after incorporating the full 3-flavor set-up.

W Boson decay : We will consider the partial decay width of the W boson into leptons and n gauge bosons

$$\Gamma_n(W^- \rightarrow L^- + \bar{\nu} + n A_X). \quad (13)$$

The constraint we will impose is that the sum of these decay widths is less than the total decay width

$$\Gamma_{\text{BSM}} \equiv \sum_{n=2}^{\infty} \Gamma_n < \Gamma_W. \quad (14)$$

For simplicity we will take $n \geq 2$ to avoid the soft divergence.

Using the Goldstone boson equivalence theorem, we find the result to leading order in m_ν to be

$$\Gamma_{\text{BSM}} = \frac{g_X^2 m_\nu^2}{1536\pi M_W} x^4 {}_2F_4(\{1, 1\}, \{2, 3, 3, 5\}, x^2) \quad (15)$$

where $x = \frac{g_X M_W}{4\pi m_X}$ and ${}_pF_q$ is the generalized hypergeometric function. In the limit of large argument, it simplifies as

$${}_2F_4(\{1, 1\}, \{2, 3, 3, 5\}, x^2) \approx \frac{16\sqrt{3}}{\pi x^{20/3}} e^{3x^{2/3}} \quad (16)$$

showing the exponential growth of the amplitudes mentioned earlier.

Bounds are obtained by requiring that this decay width is smaller than the total decay width of the W boson. For $U(1)_{L_\mu-L_\tau}$ ($U(1)_L$) we find that $m_X/g_X > 54$ MeV ($m_X/g_X > 108$ MeV). Because of the exponential, our results are insensitive to the details with which we constrain the model. For example, requiring that this decay width is smaller than 10^{-6} of the total decay width of the W boson (roughly 1 over the number of W bosons produced at LEP) tightens the above $U(1)_{L_\mu-L_\tau}$ bound to 76 MeV.

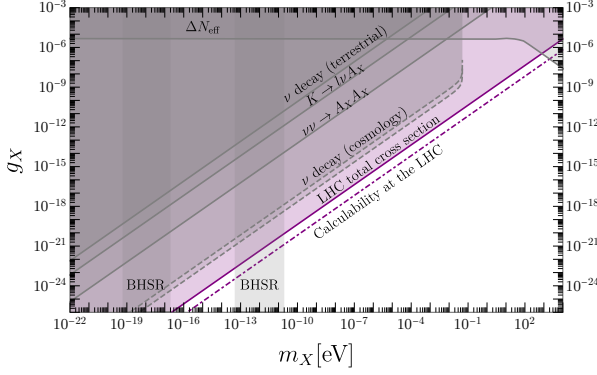


Figure 1. Low mass constraints on a Stueckelberg $U(1)_{L\mu-L\tau}$ gauge boson with Dirac neutrino masses. The purple region shows the constraint derived in Eq. (17) by demanding that multiple emission of A_X does not exceed the total inelastic cross section at the LHC. The dot-dashed purple line denotes the constraint obtained from demanding the validity of perturbation theory at the LHC, given by Eq. (18). Other constraints are from: ΔN_{eff} during BBN through thermalized A_X [34], black hole superradiance (BHSR) instability [35], rare K decays [22], ΔN_{eff} through $\nu\nu \rightarrow A_X A_X$ [22, 34], constraints on ν decay through terrestrial experiments [22, 36, 37]. We also update the cosmological constraints on ν decay as discussed in the main text, based on the recent result of Ref. [38]. Given the ν decay bounds from cosmology are model-dependent and can be relaxed, we show it via dashed lines.

LHC cross section : As can be seen in the previous analysis, the exponentially growing effects depend on the energy scale being probed and are only logarithmically sensitive to anything else. This motivates us to consider the highest energy environment on the planet, the LHC. As demonstrated before, one does not need a very sensitive probe to place a bound and we will thus be using the total inelastic cross section of the LHC.

Because the bound depends on the highest energy scale of the collision, one must understand in detail the high energy behavior of the colliding quarks. Namely, one must understand parton distribution functions (PDFs) at large energy fraction, x . The highest center of mass energy collision at the LHC was one that had a center of mass energy of ~ 8 TeV [49]. Above this, there is no experimental evidence that our PDFs are valid. Thus we will restrict our PDFs to regions of parameter space where the center of mass energy of the colliding quarks, \hat{s} , is smaller than 8 TeV.

We can calculate the center of mass cross section for $u + d \rightarrow L + \nu + n A_X$:

$$\hat{\sigma}_n = \frac{|V_{ud}|^2}{(n+2)!(n!)^2(n-1)} \left(\frac{g_2}{2\sqrt{2}} \right)^4 \left(\frac{\hat{s} g_X^2}{16\pi^2 m_X^2} \right)^n \frac{m_\nu^2}{\pi \hat{s}^2}.$$

To get the total inelastic cross section of this process, we

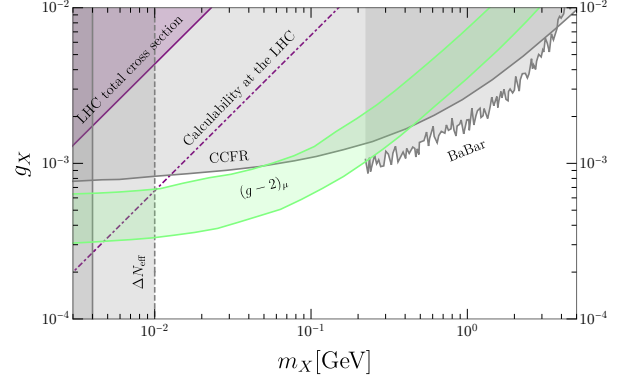


Figure 2. High mass constraints on a Stueckelberg $U(1)_{L\mu-L\tau}$ gauge boson with Dirac neutrino masses. The solid and dot-dashed purple lines are the same as in Fig. 1. Other constraints are from: ΔN_{eff} during BBN due to thermalization of A_X and entropy dump during its decay [34, 39, 40] (solid: $T_{\text{RH}} > 4$ MeV, see e.g. [41, 42]; dashed: $T_{\text{RH}} > 10$ MeV), neutrino trident process at the CCFR experiment [43, 44], and a search for $e^+e^- \rightarrow \mu^+\mu^- A_X$, $A_X \rightarrow \mu^+\mu^-$ at BaBar [45]. In the shaded green region, the muon $(g-2)$ anomaly [46, 47] can be explained by A_X at 2σ [9, 48].

integrate over the PDF and sum over n to get

$$\sigma_{\text{tot}} = \int d\hat{s} \int_{\hat{s}/s}^1 \frac{dx}{xs} \sum_{i,j,n} f_i(x) f_j \left(\frac{\hat{s}}{xs} \right) \hat{\sigma}_n (i + j \rightarrow Y),$$

where parton i and j carry momenta xP_1 and $\frac{\hat{s}}{xs}P_2$ respectively with $P_{1,2}$ being the momenta of the incoming protons and $s = (P_1 + P_2)^2 = (14 \text{ TeV})^2$ for the LHC. Y denotes a final state containing L , ν and n gauge bosons. Carrying out the integral numerically and demanding σ_{tot} to be less than the total inelastic cross section of the LHC, $\sigma = 78 \text{ mb}$ [50], we find the allowed region of $U(1)_{L\mu-L\tau}$ parameter space to be

$$m_X/g_X > 2.3 \text{ GeV}. \quad (17)$$

For $U(1)_L$ with Majorana masses we find $m_X/g_X > 4.6 \text{ GeV}$. If we instead require that the cross section is smaller than a fb, then we would obtain the exclusion 3.6(7.2) GeV for $U(1)_{L\mu-L\tau}(U(1)_L)$.

Calculability : The last bound we place is that perturbation theory at the LHC is valid. This is necessarily a somewhat fuzzy bound because the breakdown of perturbation theory is not a well defined quantity. However, it is undeniable that we can calculate observables at the LHC and so perturbation theory must be valid.

The unitarity bounds found in Eq. (8) provide a reasonable estimate for when perturbation theory breaks down. Requiring that LHC processes are calculable at a center of mass energy of 8 TeV gives the constraint

$$m_X/g_X \gtrsim 24 \text{ GeV} \quad (18)$$

for $U(1)_{L_\mu-L_\tau}$. As mentioned before, the breakdown of perturbation theory is a somewhat nebulous concept and thus this bound should be considered as more uncertain than our previous bounds.

An astute reader will notice that our previous bounds are actually weaker than this unitarity bound. As our previous bounds came from tree level calculations, they require that perturbation theory is valid. As such, strictly speaking, they only apply if the stronger calculability constraints have misestimated the breakdown of perturbation theory by about an order of magnitude.

We show our constraints visually in Fig. 1 and Fig. 2 for $U(1)_{L_\mu-L_\tau}$. We take normal ordering of the neutrino masses with the lightest neutrino being massless. As explained in the text, the bounds are not sensitive to the precise value of the mass. For other neutrino mixing parameters, we use the results from Table 3 of [51].

In Fig. 1 we have updated the cosmological bounds on these models coming from the decay of the heavier neutrinos, which requires $\tau_0 \gtrsim 4 \times 10^{5-6} \text{ sec}(m_3/50 \text{ meV})^5$ [38]. The two ν decay (cosmology) bounds represent the uncertainty in the bound on the ν lifetime. After refining the calculation of the damping of anisotropic stress due to neutrino decay and inverse decay, this new bound was obtained and found to be several orders of magnitude weaker than previous work (e.g., [52, 53]).

UV COMPLETION

Unitarity in the emission of gauge bosons can be restored by introducing the radial mode. To see the behavior of a UV completion, we consider a complex scalar Φ with charge 1 and give the neutrinos a charge $q = g_X/g$ so that the coupling of A_X to neutrinos is given by g_X while the coupling of A_X to Φ is given by g . The symmetry breaking mass term comes from the higher dimensional operator

$$V = \frac{y\Phi^q}{\Lambda^q} H L \nu^c \quad m_\nu = \frac{y v f^q}{\Lambda^q}, \quad (19)$$

which gives the standard neutrino mass term after Φ obtains a vev f . The radial mode can be partially decoupled by taking $g \rightarrow 0$ and $q, f \rightarrow \infty$ while holding $m_X = gf$ and $g_X = qg$ constant. This limit attempts to decouple the radial mode $m_\Phi \lesssim f$ but at the same time sends the symmetry breaking mass term to zero, $m_\nu \rightarrow 0$. Thus, when the neutrino mass is non-zero, the radial mode cannot be decoupled.

Using Eq. (19), one can show that the unitarity bound Λ satisfies

$$\Lambda \approx \frac{4\pi m_X}{\sqrt{27}g_X} \log^{3/2} \left(\frac{m_X}{g_X m_\nu} \right) > m_\Phi \quad (20)$$

showing that unitarity did indeed predict the correct scale of new physics in these models. In this UV theory, one can easily show that scattering involving gauge

bosons no longer grows. However, the price is that scattering involving Φ does grow. Thus this UV completion will itself require a UV completion at the scale Λ' . As this particular higher dimensional operator is identical to those seen in Froggatt–Nielsen models [54], its UV completion proceeds along a manner completely analogous to those models and will not be expounded upon here.

The importance of multiparticle emission in Stueckelberg theories could have been anticipated from this UV completion. In the UV completion, the symmetry breaking mass term arises from a higher dimensional operator of dimension $\sim q$, see Eq. (19). Discovering the bad high energy behavior of a higher dimensional operator of dimension $\sim q$ requires $\sim q$ states. The IR Stueckelberg theory should match the UV Higgs theory at the scale of the radial mode. However, because the IR Stueckelberg theory does not know which UV Higgs theory to match onto, as the energy scale becomes larger and larger, the IR theory has to match onto different UV theories with larger and larger q . Thus when scattering particles at higher and higher energies, the dominant final state involves an ever increasing number of particles.

CONCLUSION

In this letter, we considered Stueckelberg gauge bosons coupled to non-conserved currents broken by mass terms and pointed out that the production of many longitudinal modes dominates scattering and decay processes. Because of this feature, inclusive cross sections grow exponentially fast with energy. As an example, we calculated the bounds on these models coming from the total inelastic cross section of the LHC. For large gauge boson masses, these constraints are only a bit weaker than even the strongest of bounds, such as $g-2$ experiments. For most masses below a keV, these constraints are the strongest bounds on these models.

The strength of these bounds comes from the exponential growth of inclusive rates, a feature only present in the Stueckelberg limit. This growth is a double edged sword. On one hand, it allows one to use very crude measurements to place extremely stringent constraints. On the other hand, it does not benefit from precision measurements so that it is not easy to improve on the constraints without access to a higher energy environment. For example, a 100 TeV collider would improve upon the LHC bounds by about an order of magnitude.

Acknowledgments We thank Simon Knapen and Maxim Pospelov for comments on the draft. ME and AH were supported in part by the NSF grants PHY-1914480, PHY-1914731, and by the Maryland Center for Fundamental Physics (MCFP). SK was supported in part by the NSF grant PHY-1915314 and the U.S. DOE Contract DE-AC02-05CH11231. YT was also supported in part by the NSF grant PHY-2014165.

-
- * ekhtera@umd.edu
† hook@umd.edu
‡ soubhik@berkeley.edu
§ ytsai3@nd.edu
- [1] C. Boehm and Pierre Fayet, “Scalar dark matter candidates,” *Nucl. Phys. B* **683**, 219–263 (2004), [arXiv:hep-ph/0305261](#).
 - [2] Maxim Pospelov, Adam Ritz, and Mikhail B. Voloshin, “Secluded WIMP Dark Matter,” *Phys. Lett. B* **662**, 53–61 (2008), [arXiv:0711.4866 \[hep-ph\]](#).
 - [3] Nima Arkani-Hamed, Douglas P. Finkbeiner, Tracy R. Slatyer, and Neal Weiner, “A Theory of Dark Matter,” *Phys. Rev. D* **79**, 015014 (2009), [arXiv:0810.0713 \[hep-ph\]](#).
 - [4] L. F. Abbott and P. Sikivie, “A Cosmological Bound on the Invisible Axion,” *Phys. Lett. B* **120**, 133–136 (1983).
 - [5] Michael Dine and Willy Fischler, “The Not So Harmless Axion,” *Phys. Lett. B* **120**, 137–141 (1983).
 - [6] John Preskill, Mark B. Wise, and Frank Wilczek, “Cosmology of the Invisible Axion,” *Phys. Lett. B* **120**, 127–132 (1983).
 - [7] Paola Arias, Davide Cadamuro, Mark Goodsell, Joerg Jaeckel, Javier Redondo, and Andreas Ringwald, “WISPy Cold Dark Matter,” *JCAP* **06**, 013 (2012), [arXiv:1201.5902 \[hep-ph\]](#).
 - [8] Peter W. Graham, Jeremy Mardon, and Surjeet Rajendran, “Vector Dark Matter from Inflationary Fluctuations,” *Phys. Rev. D* **93**, 103520 (2016), [arXiv:1504.02102 \[hep-ph\]](#).
 - [9] S. N. Gninenko and N. V. Krasnikov, “The Muon anomalous magnetic moment and a new light gauge boson,” *Phys. Lett. B* **513**, 119 (2001), [arXiv:hep-ph/0102222](#).
 - [10] Yonatan Kahn, Michael Schmitt, and Timothy M. P. Tait, “Enhanced rare pion decays from a model of MeV dark matter,” *Phys. Rev. D* **78**, 115002 (2008), [arXiv:0712.0007 \[hep-ph\]](#).
 - [11] Maxim Pospelov, “Secluded U(1) below the weak scale,” *Phys. Rev. D* **80**, 095002 (2009), [arXiv:0811.1030 \[hep-ph\]](#).
 - [12] David Tucker-Smith and Itay Yavin, “Muonic hydrogen and MeV forces,” *Phys. Rev. D* **83**, 101702 (2011), [arXiv:1011.4922 \[hep-ph\]](#).
 - [13] Brian Batell, David McKeen, and Maxim Pospelov, “New Parity-Violating Muonic Forces and the Proton Charge Radius,” *Phys. Rev. Lett.* **107**, 011803 (2011), [arXiv:1103.0721 \[hep-ph\]](#).
 - [14] Jonathan L. Feng, Bartosz Fornal, Iftah Galon, Susan Gardner, Jordan Smolinsky, Tim M. P. Tait, and Philip Tanedo, “Particle physics models for the 17 MeV anomaly in beryllium nuclear decays,” *Phys. Rev. D* **95**, 035017 (2017), [arXiv:1608.03591 \[hep-ph\]](#).
 - [15] John Preskill, “Gauge anomalies in an effective field theory,” *Annals Phys.* **210**, 323–379 (1991).
 - [16] Pierre Fayet, “Constraints on Light Dark Matter and U bosons, from ψ , Υ , K^+ , π^0 , η and η' decays,” *Phys. Rev. D* **74**, 054034 (2006), [arXiv:hep-ph/0607318](#).
 - [17] Vernon Barger, Cheng-Wei Chiang, Wai-Yee Keung, and Danny Marfatia, “Constraint on parity-violating muonic forces,” *Phys. Rev. Lett.* **108**, 081802 (2012), [arXiv:1109.6652 \[hep-ph\]](#).
 - [18] Savely G. Karshenboim, David McKeen, and Maxim Pospelov, “Constraints on muon-specific dark forces,” *Phys. Rev. D* **90**, 073004 (2014), [Addendum: *Phys. Rev. D* **90**, 079905 (2014)], [arXiv:1401.6154 \[hep-ph\]](#).
 - [19] Jeff A. Dror, Robert Lasenby, and Maxim Pospelov, “New constraints on light vectors coupled to anomalous currents,” *Phys. Rev. Lett.* **119**, 141803 (2017), [arXiv:1705.06726 \[hep-ph\]](#).
 - [20] Jeff A. Dror, Robert Lasenby, and Maxim Pospelov, “Dark forces coupled to nonconserved currents,” *Phys. Rev. D* **96**, 075036 (2017), [arXiv:1707.01503 \[hep-ph\]](#).
 - [21] Gordan Krnjaic, Gustavo Marques-Tavares, Diego Redigolo, and Kohsaku Tobioka, “Probing Muonphilic Force Carriers and Dark Matter at Kaon Factories,” *Phys. Rev. Lett.* **124**, 041802 (2020), [arXiv:1902.07715 \[hep-ph\]](#).
 - [22] Jeff A. Dror, “Discovering leptonic forces using non-conserved currents,” *Phys. Rev. D* **101**, 095013 (2020), [arXiv:2004.04750 \[hep-ph\]](#).
 - [23] C. H. Llewellyn Smith, “High-Energy Behavior and Gauge Symmetry,” *Phys. Lett. B* **46**, 233–236 (1973).
 - [24] John M. Cornwall, David N. Levin, and George Tiktopoulos, “Uniqueness of spontaneously broken gauge theories,” *Phys. Rev. Lett.* **30**, 1268–1270 (1973), [Erratum: *Phys. Rev. Lett.* **31**, 572 (1973)].
 - [25] Satish D. Joglekar, “S matrix derivation of the Weinberg model,” *Annals Phys.* **83**, 427 (1974).
 - [26] John M. Cornwall, David N. Levin, and George Tiktopoulos, “Derivation of Gauge Invariance from High-Energy Unitarity Bounds on the s Matrix,” *Phys. Rev. D* **10**, 1145 (1974), [Erratum: *Phys. Rev. D* **11**, 972 (1975)].
 - [27] Benjamin W. Lee, C. Quigg, and H. B. Thacker, “Weak Interactions at Very High-Energies: The Role of the Higgs Boson Mass,” *Phys. Rev. D* **16**, 1519 (1977).
 - [28] Benjamin W. Lee, C. Quigg, and H. B. Thacker, “The Strength of Weak Interactions at Very High-Energies and the Higgs Boson Mass,” *Phys. Rev. Lett.* **38**, 883–885 (1977).
 - [29] Michael S. Chanowitz and Mary K. Gaillard, “The TeV Physics of Strongly Interacting W’s and Z’s,” *Nucl. Phys. B* **261**, 379–431 (1985).
 - [30] T. Appelquist and Michael S. Chanowitz, “Unitarity Bound on the Scale of Fermion Mass Generation,” *Phys. Rev. Lett.* **59**, 2405 (1987), [Erratum: *Phys. Rev. Lett.* **60**, 1589 (1988)].
 - [31] Fred Jegerlehner and Andreas Nyffeler, “The Muon g-2,” *Phys. Rept.* **477**, 1–110 (2009), [arXiv:0902.3360 \[hep-ph\]](#).
 - [32] James P. Miller, Eduardo de Rafael, B. Lee Roberts, and Dominik Stöckinger, “Muon (g-2): Experiment and Theory,” *Ann. Rev. Nucl. Part. Sci.* **62**, 237–264 (2012).
 - [33] Mark B. Wise and Yue Zhang, “Lepton Flavorful Fifth Force and Depth-dependent Neutrino Matter Interactions,” *JHEP* **06**, 053 (2018), [arXiv:1803.00591 \[hep-ph\]](#).
 - [34] Guo-yuan Huang, Tommy Ohlsson, and Shun Zhou, “Observational Constraints on Secret Neutrino Interactions from Big Bang Nucleosynthesis,” *Phys. Rev. D* **97**, 075009 (2018), [arXiv:1712.04792 \[hep-ph\]](#).
 - [35] Masha Baryakhtar, Robert Lasenby, and Mae Teo, “Black Hole Superradiance Signatures of Ultralight Vectors,” *Phys. Rev. D* **96**, 035019 (2017), [arXiv:1704.05081 \[hep-ph\]](#).
 - [36] John F. Beacom and Nicole F. Bell, “Do Solar Neutrinos Decay?” *Phys. Rev. D* **65**, 113009 (2002), [arXiv:hep-](#)

- ph/0204111.
- [37] Lena Funcke, Georg Raffelt, and Edoardo Vitagliano, “Distinguishing Dirac and Majorana neutrinos by their decays via Nambu-Goldstone bosons in the gravitational-anomaly model of neutrino masses,” *Phys. Rev. D* **101**, 015025 (2020), [arXiv:1905.01264 \[hep-ph\]](#).
 - [38] Gabriela Barenboim, Joe Zhiyu Chen, Steen Hannestad, Isabel M. Oldengott, Thomas Tram, and Yvonne Y. Y. Wong, “Invisible neutrino decay in precision cosmology,” (2020), [arXiv:2011.01502 \[astro-ph.CO\]](#).
 - [39] Ayuki Kamada and Hai-Bo Yu, “Coherent Propagation of PeV Neutrinos and the Dip in the Neutrino Spectrum at IceCube,” *Phys. Rev. D* **92**, 113004 (2015), [arXiv:1504.00711 \[hep-ph\]](#).
 - [40] Miguel Escudero, Dan Hooper, Gordan Krnjaic, and Mathias Pierre, “Cosmology with A Very Light $L_\mu - L_\tau$ Gauge Boson,” *JHEP* **03**, 071 (2019), [arXiv:1901.02010 \[hep-ph\]](#).
 - [41] Steen Hannestad, “What is the lowest possible reheating temperature?” *Phys. Rev. D* **70**, 043506 (2004), [arXiv:astro-ph/0403291](#).
 - [42] P. F. de Salas, M. Lattanzi, G. Mangano, G. Miele, S. Pastor, and O. Pisanti, “Bounds on very low reheating scenarios after Planck,” *Phys. Rev. D* **92**, 123534 (2015), [arXiv:1511.00672 \[astro-ph.CO\]](#).
 - [43] S. R. Mishra, S. A. Rabinowitz, C. Arroyo, K. T. Bachmann, R. E. Blair, C. Foudas, B. J. King, W. C. Lefmann, W. C. Leung, E. Oltman, P. Z. Quintas, F. J. Scullin, B. G. Seligman, M. H. Shaevitz, F. S. Merritt, M. J. Oreglia, B. A. Schumm, R. H. Bernstein, F. Borcharding, H. E. Fisk, M. J. Lamm, W. Marsh, K. W. B. Merritt, H. Schellman, D. D. Yovanovitch, A. Bodek, H. S. Budd, P. de Barbaro, W. K. Sakumoto, P. H. Sandler, and W. H. Smith, “Neutrino tridents and w-z interference,” *Phys. Rev. Lett.* **66**, 3117–3120 (1991).
 - [44] Wolfgang Altmannshofer, Stefania Gori, Maxim Pospelov, and Itay Yavin, “Neutrino Trident Production: A Powerful Probe of New Physics with Neutrino Beams,” *Phys. Rev. Lett.* **113**, 091801 (2014), [arXiv:1406.2332 \[hep-ph\]](#).
 - [45] J. P. Lees *et al.* (BaBar), “Search for a muonic dark force at BABAR,” *Phys. Rev. D* **94**, 011102 (2016), [arXiv:1606.03501 \[hep-ex\]](#).
 - [46] G. W. Bennett *et al.* (Muon g-2), “Final Report of the Muon E821 Anomalous Magnetic Moment Measurement at BNL,” *Phys. Rev. D* **73**, 072003 (2006), [arXiv:hep-ex/0602035](#).
 - [47] T. Aoyama *et al.*, “The anomalous magnetic moment of the muon in the Standard Model,” *Phys. Rept.* **887**, 1–166 (2020), [arXiv:2006.04822 \[hep-ph\]](#).
 - [48] Seungwon Baek, N. G. Deshpande, X. G. He, and P. Ko, “Muon anomalous g-2 and gauged $L(\mu\text{on}) - L(\tau\text{au})$ models,” *Phys. Rev. D* **64**, 055006 (2001), [arXiv:hep-ph/0104141](#).
 - [49] Albert M Sirunyan *et al.* (CMS), “Search for high mass dijet resonances with a new background prediction method in proton-proton collisions at $\sqrt{s} = 13$ TeV,” *JHEP* **05**, 033 (2020), [arXiv:1911.03947 \[hep-ex\]](#).
 - [50] M. Aaboud *et al.* (ATLAS), “Measurement of the Inelastic Proton-Proton Cross Section at $\sqrt{s} = 13$ TeV with the ATLAS Detector at the LHC,” *Phys. Rev. Lett.* **117**, 182002 (2016), [arXiv:1606.02625 \[hep-ex\]](#).
 - [51] Ivan Esteban, M. C. Gonzalez-Garcia, Michele Maltoni, Thomas Schwetz, and Albert Zhou, “The fate of hints: updated global analysis of three-flavor neutrino oscillations,” *JHEP* **09**, 178 (2020), [arXiv:2007.14792 \[hep-ph\]](#).
 - [52] Maria Archidiacono and Steen Hannestad, “Updated constraints on non-standard neutrino interactions from Planck,” *JCAP* **07**, 046 (2014), [arXiv:1311.3873 \[astro-ph.CO\]](#).
 - [53] Miguel Escudero and Malcolm Fairbairn, “Cosmological Constraints on Invisible Neutrino Decays Revisited,” *Phys. Rev. D* **100**, 103531 (2019), [arXiv:1907.05425 \[hep-ph\]](#).
 - [54] C. D. Froggatt and Holger Bech Nielsen, “Hierarchy of Quark Masses, Cabibbo Angles and CP Violation,” *Nucl. Phys. B* **147**, 277–298 (1979).
 - [55] Spencer Chang and Markus A. Luty, “The Higgs Trilinear Coupling and the Scale of New Physics,” *JHEP* **03**, 140 (2020), [arXiv:1902.05556 \[hep-ph\]](#).
 - [56] Fayez Abu-Ajamieh, Spencer Chang, Miranda Chen, and Markus A. Luty, “Higgs Coupling Measurements and the Scale of New Physics,” (2020), [arXiv:2009.11293 \[hep-ph\]](#).
 - [57] K. Kovarik *et al.*, “nCTEQ15 - Global analysis of nuclear parton distributions with uncertainties in the CTEQ framework,” *Phys. Rev. D* **93**, 085037 (2016), [arXiv:1509.00792 \[hep-ph\]](#).
 - [58] D. B. Clark, E. Godat, and F. I. Olness, “ManeParse : A Mathematica reader for Parton Distribution Functions,” *Comput. Phys. Commun.* **216**, 126–137 (2017), [arXiv:1605.08012 \[hep-ph\]](#).

Bounds on Gauge Bosons Coupled to Non-conserved Currents

Supplementary Material

Majid Ekhterachian, Anson Hook, Soubhik Kumar, Yuhsin Tsai

This Supplementary Material contains additional calculations supporting the results in the main text.

UNITARITY BOUNDS - n -TO- n SCATTERING

When discussing our unitarity bounds, we will follow the conventions and discussions of Ref. [55, 56] and for simplicity we will be working in the limit of massless particles. Any S matrix can be decomposed into $S = \mathbf{1} + iT$. The identity matrix describes the situation where particles pass by without interacting while the transition matrix T describes nontrivial processes. The states we will be considering have a continuous label P , the total momentum, and discrete labels α . These states are normalized as

$$\langle P', \alpha' | P, \alpha \rangle = (2\pi)^4 \delta^4(P - P') \delta_{\alpha\alpha'}. \quad (\text{S1})$$

The amplitude $\hat{\mathbf{M}}$ is defined by

$$\langle P', \alpha' | T | P, \alpha \rangle = (2\pi)^4 \delta^4(P - P') \hat{\mathbf{M}}_{\alpha\alpha'} \quad \langle P', \alpha' | S | P, \alpha \rangle = (2\pi)^4 \delta^4(P - P') S_{\alpha\alpha'}. \quad (\text{S2})$$

The main result that we will use is that $|\hat{\mathbf{M}}_{\alpha\alpha'}| \leq 1$ for all α and α' at tree level. When $\alpha \neq \alpha'$, this statement follows directly from the conservation of probability. For $\alpha = \alpha'$ we use unitarity

$$1 = \delta_{\alpha\alpha} = \sum_{\gamma} S_{\alpha\gamma}^\dagger S_{\gamma\alpha} = 1 - 2 \text{Im} \hat{\mathbf{M}}_{\alpha\alpha} + \sum_{\gamma} |\hat{\mathbf{M}}_{\gamma\alpha}|^2. \quad (\text{S3})$$

From this we have

$$2 \text{Im} \hat{\mathbf{M}}_{\alpha\alpha} = \sum_{\gamma} |\hat{\mathbf{M}}_{\gamma\alpha}|^2 \geq |\hat{\mathbf{M}}_{\alpha\alpha}|^2 \quad (\text{S4})$$

which can be massaged into the form $1 \geq |\text{Re} \hat{\mathbf{M}}_{\alpha\alpha}|^2 + |\text{Im} \hat{\mathbf{M}}_{\alpha\alpha} - 1|^2$. From this we see that $|\text{Re} \hat{\mathbf{M}}_{\alpha\alpha}| \leq 1$. Since $\hat{\mathbf{M}}_{\alpha\alpha}$ is real at tree level, we have $|\hat{\mathbf{M}}_{\alpha\alpha}| \leq 1$.

We now have the unitarity bound $|\hat{\mathbf{M}}_{\alpha\alpha'}| \leq 1$ so we can apply it to the theory described in Eq. (4). We will be considering the initial and final states each with a neutrino ν and n Goldstone bosons ϕ . We define our states as

$$|P, n, \alpha\rangle = C_n \int d^4x e^{-iPx} \phi^{(-)}(x)^n \nu_\alpha^{(-)}(x) |0\rangle \quad (\text{S5})$$

where C_n is a normalization constant, $(-)$ are the part of the fields that contain the creation operators, and α is the spinor index of the fermion. These states are normalized as

$$\langle P', n', \dot{\alpha} | P, n, \alpha \rangle = (2\pi)^4 \delta^4(P - P') \delta_{nn'} \frac{\not{p}^{\alpha\dot{\alpha}}}{E} \quad (\text{S6})$$

where E is the total energy. This normalization was chosen to reproduce Eq. (S1) in the center of mass frame, which we will be using from here on. From this, we have the normalization constant

$$\frac{1}{|C_n|^2} = \frac{1}{2(n+1)(n-1)!} \left(\frac{E}{4\pi} \right)^{2n-1}. \quad (\text{S7})$$

We can finally calculate the amplitude of interest using Eq. (5) to give

$$\langle P', n, \alpha | (-i) \int d^4x \bar{\nu}(x) \frac{m_\nu}{(2n)!} \left(\frac{ig_X P_L \phi(x)}{m_X} \right)^{2n} \nu(x) | P, n, \alpha \rangle = (2\pi)^4 \delta^4(P - P') i \hat{\mathbf{M}}(\nu + n\phi \rightarrow \nu + n\phi) \quad (\text{S8})$$

$$|\hat{\mathbf{M}}(\nu + n\phi \rightarrow \nu + n\phi)| = \frac{g_X m_\nu}{2m_X (n+1)! n! (n-1)!} \left(\frac{g_X E}{4\pi m_X} \right)^{2n-1} \quad (\text{S9})$$

Imposing $|\hat{\mathbf{M}}| \leq 1$ gives the results shown in the text. For reference, the amplitude $\hat{\mathbf{M}}$ is related to the more familiar matrix element \mathcal{M} by normalization constants and phase space integrals

$$\hat{\mathbf{M}}_{\alpha\alpha'} = C_\alpha^* C_{\alpha'} \int d\Phi_\alpha d\Phi_{\alpha'} \mathcal{M}_{\alpha\alpha'}. \quad (\text{S10})$$

The phase space differentials $d\Phi_\alpha$ will be given below.

UNITARITY BOUNDS ON AN ANOMALOUS $U(1)$

In this section we calculate the unitarity bounds on an anomalous gauge theory in a manner analogous to what we did for n -to- n scattering. We leave unitarity gauge by a gauge transformation ϕ/m_X . Because the theory is anomalous, an anomaly term is added to the Lagrangian

$$\mathcal{L} \supset \frac{g^2 \mathcal{A}}{32\pi^2} \frac{g_X \phi}{m_X} W^a \tilde{W}^a, \quad (\text{S11})$$

where $\tilde{W}^{\mu\nu} = \frac{1}{2} \epsilon^{\mu\nu\rho\sigma} W_{\rho\sigma}$ and W^a are the gauge bosons with which $U(1)_X$ is anomalous and \mathcal{A} is the anomaly coefficient.

We will consider 2-to-2 scattering of W^1 gauge bosons via the Goldstone boson ϕ , which contains all of the leading high energy behavior in Feynman-'t Hooft gauge. The largest amplitude occurs when all four gauge bosons have the same helicity. A short calculation gives the amplitude

$$|\hat{\mathbf{M}}(W^1 + W^1 \rightarrow W^1 + W^1)| = \frac{s}{4\pi} \left(\frac{g_X}{m_X} \frac{g^2 \mathcal{A}}{32\pi^2} \right)^2 \quad (\text{S12})$$

Requiring the unitarity bound $|\hat{\mathbf{M}}| < 1$ be saturated at the center of mass energy Λ_a , we arrive at the result

$$\Lambda_a = \frac{\sqrt{4\pi} m_X}{g_X} \frac{32\pi^2}{g^2 \mathcal{A}}. \quad (\text{S13})$$

DECAY WIDTH OF THE W BOSON

Here we compute the decay width of the W boson into a lepton, a neutrino and n gauge bosons. The decay is dominated by the decay into longitudinal modes which we calculate using the Goldstone boson equivalence theorem.

The relevant process is shown in Fig. S1. We denote the four momenta of the W boson, the outgoing lepton l ,

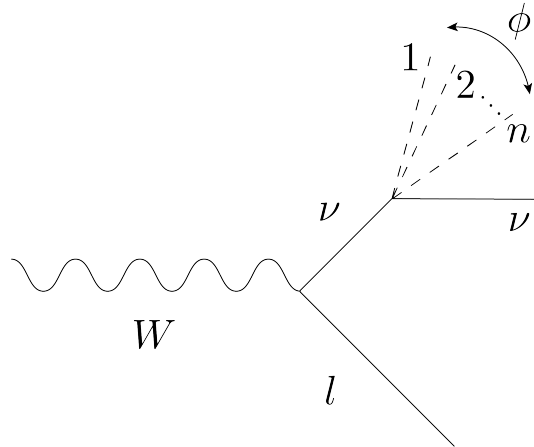


Figure S1. The decay $W \rightarrow n\phi + l + \nu$.

the intermediate neutrino and the outgoing neutrino as p_W , p_l , q and p_ν , respectively. We also denote the collective momenta of the n Goldstone bosons ϕ as $p_\phi = p_1 + p_2 + \dots + p_n$. We will ignore the masses of ϕ , ν and l throughout

our calculation, except those appearing in the neutrino-Goldstone boson coupling. We will consider a single neutrino flavor, and later generalize to the standard three-flavor structure. The matrix element is

$$i\mathcal{M} = - \left(\frac{g_2}{2\sqrt{2}} \right) \bar{u}(p_l) \gamma_\alpha (1 - \gamma_5) \epsilon^\alpha \frac{i \not{q}}{q^2} \kappa_n v(p_\nu), \quad (\text{S14})$$

where κ_n denotes the coupling of neutrinos to n -Goldstone bosons, obtained from Eq. (5). We see that $\kappa_n \propto \gamma_5$ for odd values of n . However, it can be checked that $i\mathcal{M}$ is the same for both even and odd values of n . The amplitude can be squared to give

$$\frac{1}{3} \sum |\mathcal{M}|^2 = \frac{2}{3} \left(\frac{g_2 \kappa_n}{2\sqrt{2}} \right)^2 \text{Tr} \left[\gamma^\beta \not{p}_l \gamma^\alpha \not{q} \not{p}_\nu \not{q} (1 + \gamma_5) \right] \frac{1}{q^4} \Pi_{\alpha\beta}, \quad (\text{S15})$$

where $\Pi_{\alpha\beta} = \left(-g_{\alpha\beta} + \frac{p_W^\alpha p_W^\beta}{M_W^2} \right)$. The factor of $1/3$ comes from averaging over initial W polarizations. After some algebra this can be reduced to,

$$\frac{1}{3} \sum |\mathcal{M}|^2 = \left(\frac{g_2 \kappa_n}{2\sqrt{2}} \right)^2 \frac{1}{3q^4} (8g^{\alpha\beta} [q^2(p_l \cdot p_\nu) - 2(q \cdot p_\nu)(q \cdot p_l)] + 32(q \cdot p_\nu)p_l^\alpha q^\beta - 16q^2 p_l^\alpha p_\nu^\beta) \Pi_{\alpha\beta}. \quad (\text{S16})$$

Let us now integrate over the phase space of the n ϕ and the outgoing neutrino. To this end, we will use the following identities involving k -body phase space of massless particles [56],

$$\Phi_k(P) = \int d\Phi_k(P) \equiv \int \frac{d^3 p_1}{(2\pi)^3} \frac{1}{2E_1} \cdots \frac{d^3 p_k}{(2\pi)^3} \frac{1}{2E_k} (2\pi)^4 \delta^4(p_1 + \cdots + p_k - P) = \frac{1}{8\pi(k-1)!(k-2)!} \left(\frac{E}{4\pi} \right)^{2k-4}, \quad (\text{S17})$$

$$\int d\Phi_k(P) p_1^\mu = \frac{1}{k} \Phi_k(P) P^\mu, \quad (\text{S18})$$

$$\int d\Phi_k(P) p_1 \cdot p_2 = \frac{1}{2 \binom{k}{2}} \Phi_k(P) P^2, \quad (\text{S19})$$

with $E = \sqrt{P^2}$ being the center of mass energy. Utilizing the above identities and doing the contraction with $\Pi_{\alpha\beta}$ we get,

$$\begin{aligned} \int d\Phi_{n+1}(q) \left(\frac{1}{3} \sum |\mathcal{M}|^2 \right) &= \frac{8}{3q^2} \left(\frac{g_2 \kappa_n}{2\sqrt{2}} \right)^2 \left[(p_l \cdot q) + \frac{2(p_W \cdot q)(p_l \cdot p_W)}{M_W^2} \right] \frac{\Phi_{n+1}(q)}{(n+1)}, \\ &= \left(\frac{g_2 \kappa_n}{2\sqrt{2}} \right)^2 \frac{q^{2n-4}}{3\pi(n+1)!(n-1)!} \frac{1}{(4\pi)^{2n-2}} \left(3(p_W \cdot p_l) - \frac{2(p_W \cdot p_l)^2}{M_W^2} \right). \end{aligned} \quad (\text{S20})$$

As a final step, we go to the rest frame of the W and integrate over the lepton momenta to get,

$$\Gamma(W \rightarrow l + \nu + n\phi) = \frac{g_2^2 M_W^{2n-1} \kappa_n^2}{(4\pi)^{2n}} \frac{1}{16\pi(n!)^2(n+2)!(n-1)} \quad \text{for } n > 1. \quad (\text{S21})$$

Here we have also multiplied by a factor of $1/n!$ to account for the n identical ϕ s in the final state. The total decay width of the W -boson into a final state containing an arbitrary number of ϕ s is then obtained after summing over n ,

$$\Gamma_{\text{BSM}} \equiv \sum_{n>1} \Gamma(W \rightarrow l + \nu + n\phi) = \frac{1}{16\pi \times 96} \frac{g_2^2 m_\nu^2}{M_W} \left(\frac{M_W g_X}{4\pi m_X} \right)^4 {}_2F_4 \left(\{1, 1\}, \{2, 3, 3, 5\}, \left(\frac{M_W g_X}{4\pi m_X} \right)^2 \right). \quad (\text{S22})$$

The $n = 1$ case is special as there is a soft divergence leading to a log enhancement of the form $\log(m_W/m_X)$. As this log is only present for $n = 1$, we conservatively neglect the $n = 1$ contribution to the decay width.

PRODUCTION OF GAUGE BOSONS AT THE LHC

Now we focus on the diagram in Fig. S2. We use the same notation for various momenta as before, and also denote the momenta of u and d quarks by p_u and p_d respectively. The matrix element is given by,

$$i\mathcal{M} = i \left(\frac{g_2}{2\sqrt{2}} \right)^2 V_{ud}^* \kappa_n [\bar{v}(p_u) \gamma_\mu (1 - \gamma_5) u(p_d)] \frac{-i \left(g^{\mu\nu} - \frac{p_W^\mu p_W^\nu}{M_W^2} \right)}{p_W^2 - M_W^2} \left[\bar{u}(p_l) \gamma_\nu (1 - \gamma_5) \frac{i}{\not{q}} v(p_\nu) \right], \quad (\text{S23})$$

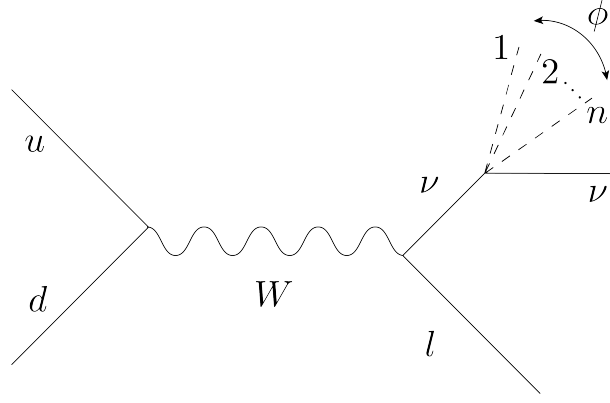


Figure S2. The parton level scattering $u + d \rightarrow W^* \rightarrow n \phi + l + \nu$.

where V_{ud} is the CKM matrix element. After some algebra the matrix element squared can be reduced to,

$$|\mathcal{M}|^2 = 64 \left(\frac{g_2}{2\sqrt{2}} \right)^4 |V_{ud}|^2 \frac{\kappa_n^2}{q^4} (p_{u\nu} p_{d\beta} + p_{d\nu} p_{u\beta} - (p_u \cdot p_d) g_{\nu\beta} + i\epsilon_{\rho\nu\sigma\beta} p_u^\rho p_d^\sigma) L^{\nu\beta}, \quad (\text{S24})$$

where the quantity $L^{\nu\beta}$ is given by,

$$L^{\nu\beta} = 2(q \cdot p_\nu) (2p_l^\nu q^\beta - g^{\nu\beta} (p_l \cdot q)) - q^2 (2p_l^\nu p_\nu^\beta - g^{\nu\beta} (p_l \cdot p_\nu)) + i\epsilon^{\gamma\nu\delta\beta} (2(q \cdot p_\nu) p_{l\gamma} q_\delta - q^2 p_{l\gamma} p_{\nu\delta}). \quad (\text{S25})$$

We can now do the $(n+1)$ -dimensional phase space integral over the scalar and neutrino momenta,

$$\int d\Phi_{n+1} L^{\nu\beta} = q^2 \frac{\Phi_{n+1}}{n+1} ((2p_l^\nu q^\beta - g^{\nu\beta} (p_l \cdot q)) + i\epsilon^{\gamma\nu\delta\beta} q^2 p_{l\gamma} q_\delta). \quad (\text{S26})$$

Averaging over initial spin and multiplying by $1/n!$ to account for identical particles in the final state we then get,

$$\int d\Phi_{n+1} \left(\frac{1}{4} \sum |\mathcal{M}|^2 \right) = 64 \left(\frac{g_2}{2\sqrt{2}} \right)^4 |V_{ud}|^2 \kappa_n^2 \frac{\Phi_{n+1}}{(n+1)!} \frac{(p_l \cdot p_u)(q \cdot p_d)}{q^2(\hat{s} - M_W^2)^2}. \quad (\text{S27})$$

Here $\hat{s} = p_W^2$ is the parton center-of-mass (COM) energy. To proceed further, it is useful to go to the parton COM frame. Then integrating over the lepton momenta we get the differential cross-section for emitting n Goldstone bosons,

$$\begin{aligned} \hat{\sigma}_n(u + d \rightarrow W^* \rightarrow l + \nu + n\phi) &= \frac{1}{8E_u E_d} \frac{1}{\pi^2} \frac{1}{(4\pi)^{2n-2}} \left(\frac{g_2}{2\sqrt{2}} \right)^4 \kappa_n^2 |V_{ud}|^2 \frac{\hat{s}^{n+1}}{(n-1)n(n+2)!} \frac{1}{(\hat{s} - M_W^2)^2} \frac{1}{8\pi n!(n-1)!}, \\ &\simeq \frac{1}{(n+2)!(n!)^2(n-1)} \left(\frac{g_2}{2\sqrt{2}} \right)^4 |V_{ud}|^2 \left(\frac{\hat{s} g_X^2}{16\pi^2 m_X^2} \right)^n \frac{m_\nu^2}{\pi \hat{s}^2} \quad \text{for } n > 1. \end{aligned} \quad (\text{S28})$$

In the last step above, we have used $\hat{s} \gg M_W^2$ since the strongest constraints come from when \hat{s} is large. To get the total rate for emission of gauge bosons we sum over n to get,

$$\hat{\sigma}_{\text{parton}} = \sum_{n \geq 1} \hat{\sigma}_n = \left(\frac{g_2}{2\sqrt{2}} \right)^4 |V_{ud}|^2 \frac{m_\nu^2}{96\pi \hat{s}^2} \left(\frac{\sqrt{\hat{s}} g_X}{4\pi m_X} \right)^4 {}_2F_4 \left(1, 1; 2, 3, 3, 5; \left(\frac{\sqrt{\hat{s}} g_X}{4\pi m_X} \right)^2 \right). \quad (\text{S29})$$

From the above parton-level cross-section, we can derive the physical cross-section by including the appropriate parton distribution functions (PDF) f_i ,

$$\sigma_{\text{tot}} = \int d\hat{s} \int_{\hat{s}/s}^1 \frac{dx}{xs} \sum_{i,j} f_i(x) f_j \left(\frac{\hat{s}}{xs} \right) \hat{\sigma}_{\text{parton}} \left(i(xP_1) + j \left(\frac{\hat{s}}{xs} P_2 \right) \rightarrow Y \right). \quad (\text{S30})$$

Here Y denotes the final state under consideration, and P_1, P_2 are the proton momenta with i, j running over different parton initial states. The proton COM energy is given by $s = 14$ TeV. We use the **nCTEQ15** PDF set [57] and the **ManeParse** package [58] to carry out the PDF integrals above.